

X-ray and neutron powder diffraction studies of $(\text{Ba}_{1-x}\text{Sr}_x)\text{Y}_2\text{CuO}_5$

Z. Yang, W. Wong-Ng, and L. P. Cook

Ceramics Division, Materials Science and Engineering Laboratory, National Institute of Standards and Technology, Gaithersburg, Maryland 20899

J. A. Kaduk

BP-Amoco Chemicals, Naperville, Illinois 60566

Q. Z. Huang

NIST Center for Neutron Research, National Institute of Standards and Technology, Gaithersburg, Maryland 20899

(Received 26 October 2005; accepted 23 May 2006)

This paper reports the results of crystallography and crystal chemistry investigation of the $(\text{Ba}_{1-x}\text{Sr}_x)\text{Y}_2\text{CuO}_5$ (“green phase”) solid solution series by X-ray powder diffraction (XPD) and neutron powder diffraction techniques. The single phase regions for $(\text{Ba}_{1-x}\text{Sr}_x)\text{Y}_2\text{CuO}_5$ were determined to be $0 \leq x \leq 0.3$ for samples prepared at 810 °C in 100 Pa p_{O_2} , and $0 \leq x \leq 0.7$ for samples prepared at 930 °C in air. All single phase $(\text{Ba}_{1-x}\text{Sr}_x)\text{Y}_2\text{CuO}_5$ samples are isostructural to BaY_2CuO_5 and can be indexed using an orthorhombic cell with the space group Pnma. Lattice parameters, a, b, c and the cell volume, V , of the $(\text{Ba}_{1-x}\text{Sr}_x)\text{Y}_2\text{CuO}_5$ members decrease linearly with increasing Sr substitution (x) on the Ba site. The general structure of $(\text{Ba}_{1-x}\text{Sr}_x)\text{Y}_2\text{CuO}_5$ can be considered as having a three-dimensional interconnected network of $[\text{YO}_7]$, $[(\text{Ba}, \text{Sr})\text{O}_{11}]$, and $[\text{CuO}_5]$ polyhedra. The copper ions are located inside distorted $[\text{CuO}_5]$ “square” pyramids. These pyramids are connected by the $[\text{Y}_2\text{O}_{11}]$ groups that are formed from two mon capped $[\text{YO}_7]$ trigonal prisms sharing a triangular face. The Ba^{2+} ions are found to reside in distorted 11-fold coordinated cages. The oxygen sites are essentially fully occupied. XPD reference patterns of two members of the series, $(\text{Ba}_{0.3}\text{Sr}_{0.7})\text{Y}_2\text{CuO}_5$ and $(\text{Ba}_{0.7}\text{Sr}_{0.3})\text{Y}_2\text{CuO}_5$, were prepared for inclusion in the powder diffraction file. © 2006 International Centre for Diffraction Data.

[DOI: 10.1154/1.2217029]

Key words: $(\text{Ba}_{1-x}\text{Sr}_x)\text{Y}_2\text{CuO}_5$, Rietveld refinements, X-ray and neutron powder diffraction, crystal structure and crystal chemistry, X-ray reference powder diffraction patterns

I. INTRODUCTION

The development of coated conductor technology has moved forward at a rapid pace in recent years (Paranthaman and Izumi, 2004). High-quality textured conductors have been successfully produced in long-lengths with various state-of-the-art techniques, including electron-beam deposition (Feenstra *et al.*, 1991; Feenstra 1999; Solovyov *et al.*, 1998; Wu *et al.*, 2001), metalorganic chemical vapor deposition (Selvamanickam *et al.*, 2004), pulsed laser deposition (Usoskin and Freyhardt, 2004), and open-air solution methods (Rupich *et al.*, 2004; McIntyre *et al.*, 1995; Yoshizumi *et al.*, 2004). Commercialized practical applications of these conductors are within reach in the near future.

The state-of-the-art technologies for producing textured coated conductors are ion beam assisted deposition (IBAD) (Iijima *et al.*, 2004; Reade *et al.*, 1992; Foltyn *et al.*, 1993; Arendt and Foltyn, 2004), rolling assisted biaxially textured substrate (RABiTS) (Goyal *et al.*, 2004; Malozemoff *et al.*, 2000; Paranthaman *et al.*, 2000; Goyal *et al.*, 2001; Aytug *et al.*, 2003), Paranthaman *et al.*, 1997), and to a smaller extent, the inclined substrate deposition (ISD) technique (Bauer *et al.*, 1999; Balachandran and Chudzik, 2002). As with all high- T_c applications, the issues of cost and performance are intimately linked to the optimized processing of these materials. All the IBAD, RABiTS, and ISD methods

involve deposition of $\text{Ba}_2\text{YCu}_3\text{O}_{6+z}$ (Y)-213 or $\text{Ba}_2\text{RCu}_3\text{O}_{6+z}$ (R-213) films on biaxially textured buffered substrates. For example, typically an IBAD buffered substrate consists of a layer, such as SrTiO_3 , sandwiched between a Ni-alloyed substrate and a Y-213 layer. Therefore, an understanding of the interaction between the buffer layer and the superconductor phase is imperative for the processing of these tapes.

One of our current projects is to characterize the reaction products of the interactions between Y-213 and SrTiO_3 . Since BaY_2CuO_5 is known as the impurity “green phase” (Wong-Ng *et al.*, 1989; Wong-Ng *et al.*, 1995; Watkins *et al.*, 1988; Michel and Raveau, 1982; Hazen *et al.*, 1987; Hsu *et al.*, 1996; Ross *et al.*, 1987; Fjellvag *et al.*, 1987; Sato and Nakada, 1989; Hunter *et al.*, 1989; Salinas-Sanchez *et al.*, 1992; Buttner and Maslen, 1993; Shaked *et al.*, 1993) during processing of Y-213, Sr-doped BaY_2CuO_5 is also one of the potential interaction products. The goal of this paper is to characterize the $(\text{Ba}_{1-x}\text{Sr}_x)\text{Y}_2\text{CuO}_5$ solid solution series, including the homogeneity range, crystal structural trend, and crystal chemistry of the members due to the substitution of Ba by Sr. The characterization techniques include X-ray powder diffraction (XPD) and neutron powder diffraction (NPD). Since X-ray reference powder diffraction patterns are critical for phase characterization, we have also prepared powder patterns of selected $(\text{Ba}_{1-x}\text{Sr}_x)\text{Y}_2\text{CuO}_5$ phases for inclusion in the powder diffraction file (PDF).

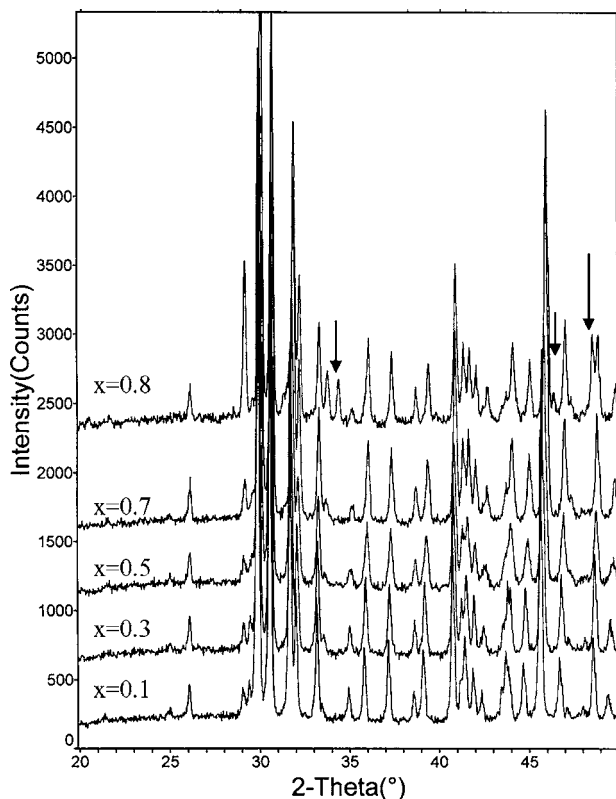


Figure 1. XPD patterns for $(\text{Ba}_{1-x}\text{Sr}_x)\text{Y}_2\text{CuO}_5$ prepared at 930 °C (in air). The presence of peaks due to second phase impurities, such as Y_2O_3 , is indicated by arrows in the pattern of $x=0.8$.

II. EXPERIMENTAL

A. Sample preparation

Certain commercial equipment, instruments, or materials are identified in this paper to foster understanding. Such identification does not imply recommendation or endorsement by the National Institute of Standards and Technology, nor does it imply that the materials or equipment identified are necessarily the best available for the purpose. Two series of $(\text{Ba}_{1-x}\text{Sr}_x)\text{Y}_2\text{CuO}_5$ samples ($x=0.1, 0.2, 0.3, 0.4, 0.5, 0.6, 0.7, 0.8$, and 0.9) were prepared using the high-temperature solid-state technique. One series was prepared in air, while the other one was in 100 Pa p_{O_2} in Ar by volume (or 0.1% O_2). According to the stoichiometric ratios, the mixtures of Y_2O_3 (99.999%), CuO (99.99%), SrCO_3 (99.99%), and BaCO_3 (99.99%) were first heat treated at 750 °C for 5 h to

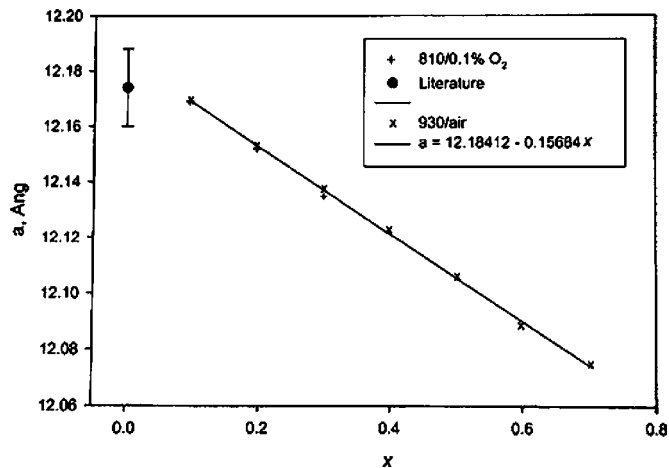


Figure 2. Variation of lattice parameter a versus composition (x) in $(\text{Ba}_{1-x}\text{Sr}_x)\text{Y}_2\text{CuO}_5$. The solid dot refers to the average literature a value for BaY_2CuO_5 (Wong-Ng *et al.*, 1989; Wong-Ng *et al.*, 1995; Watkins *et al.*, 1988; Michel and Raveau, 1982; Hazen *et al.*, 1987; Hsu *et al.*, 1996; Ross *et al.*, 1987; Fjellvag *et al.*, 1987; Sato and Nakada, 1989; Hunter *et al.*, 1989; Salinas-Sanchez *et al.*, 1992; Buttner and Maslen, 1993; Shaked *et al.*, 1993), with standard deviation (1 sigma) indicated.

decompose the carbonates, and then reground and reheated at 930 °C (in air) and 810 °C (100 Pa p_{O_2}), respectively, for 21 days with intermediate grindings and pelletizations. The annealing process was repeated until no further changes were detected in the powder X-ray diffraction patterns.

Phase analyses were carried out using a Phillips X-ray powder diffractometer with $\text{Cu } K\alpha$ radiation and equipped with a series of Soller slits and a scintillation counter. The 2θ scanning range was from 3° to 66°, and the step interval was 0.03°. The reference diffraction pattern of BaY_2CuO_5 (PDF 38-1434) (ICDD, 1987) was used for performing phase identification.

B. X-ray reference powder diffraction patterns

The green $(\text{Ba}_{1-x}\text{Sr}_x)\text{Y}_2\text{CuO}_5$ powders were mounted in zero-background quartz holders with double-sided adhesive tape. A Scintag PAD V diffractometer equipped with an Ortec intrinsic Ge detector was used to measure the powder patterns ($\text{Cu } K\alpha$ radiation, 40 kV, 30 mA) from 3° to 140° 2θ in 0.02° steps, counting for 10 s per step.

TABLE I. Refined lattice parameters of the orthorhombic $(\text{Ba}_{1-x}\text{Sr}_x)\text{Y}_2\text{CuO}_5$ compounds (space group Pnma); the average lattice parameters of BaY_2CuO_5 from 11 literature sources (Wong-Ng *et al.*, 1989; Wong-Ng *et al.*, 1995; Watkins *et al.*, 1988; Michel and Raveau, 1982; Hazen *et al.*, 1987; Hsu *et al.*, 1996; Ross *et al.*, 1987; Fjellvag *et al.*, 1987; Sato and Nakada, 1989; Hunter *et al.*, 1989; Salinas-Sanchez *et al.*, 1992; Buttner and Maslen, 1993; Shaked *et al.*, 1993) are $a=12.174(14)$ Å, $b=5.657(3)$ Å, $c=7.131(3)$ Å, $V=491.28(71)$ Å³.

x	0.10		0.20		0.30		0.40		0.50		0.60		0.70	
	810 °C 100 Pa p_{O_2}	930 °C air	810 °C 100 Pa p_{O_2}	930 °C air	810 °C 100 Pa p_{O_2}	930 °C air								
a, Å	12.16681(5)	12.16747(7)	12.15093(5)	12.15212(7)	12.1343(1)	12.13823(7)	12.1237(1)	12.1062(2)	12.0865(1)	12.0754(1)				
b, Å	5.65359(2)	5.65369(3)	5.64680(2)	5.64749(2)	5.63980(4)	5.64147(2)	5.63510(8)	5.6280(1)	5.61929(5)	5.61419(5)				
c, Å	7.13120(3)	7.13129(4)	7.12736(3)	7.12803(4)	7.12294(6)	7.12493(3)	7.1211(1)	7.1160(1)	7.11031(6)	7.10741(6)				
V, Å ³	490.530(4)	490.569(5)	489.036(5)	489.190(5)	487.460(7)	487.898(4)	486.50(1)	484.84(1)	482.916(8)	481.839(7)				

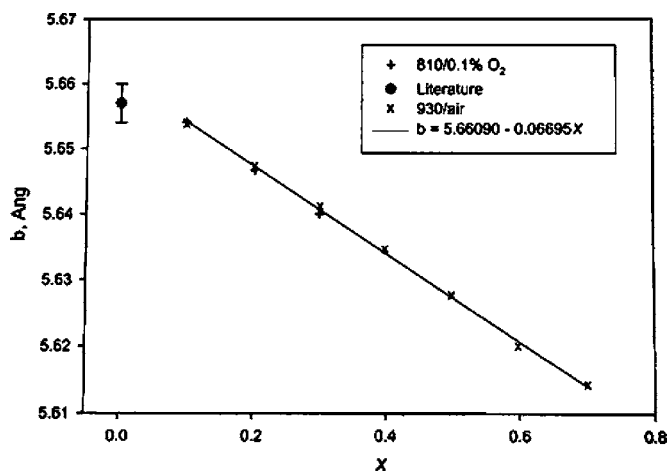


Figure 3. Variation of lattice parameter b versus composition (x) in $(\text{Ba}_{1-x}\text{Sr}_x)\text{Y}_2\text{CuO}_5$. The solid dot refers to the average literature b value for BaY_2CuO_5 (Wong-Ng *et al.*, 1989; Wong-Ng *et al.*, 1995; Watkins *et al.*, 1988; Michel and Raveau, 1982; Hazen *et al.*, 1987; Hsu *et al.*, 1996; Ross *et al.*, 1987; Fjellvag *et al.*, 1987; Sato and Nakada, 1989; Hunter *et al.*, 1989; Salinas-Sanchez *et al.*, 1992; Buttner and Maslen, 1993; Shaked *et al.*, 1993), with standard deviation (1 sigma) indicated.

All data processing and structural refinements were carried out using the GSAS Suite of Rietveld software (Larson and von Dreele, 1985; Rietveld, 1969). The reported structure of BaY_2CuO_5 (Watkins *et al.*, 1988) was employed as a starting model. Included in the refinements were the atomic coordinates and isotropic displacement coefficients, a scale factor, a sample displacement coefficient, and the lattice parameters. The peak profiles were described using a pseudo-Voigt function; only the Cauchy Y (strain) terms were refined. The backgrounds were described using a three-term cosine Fourier series.

X-ray reference powder patterns of $(\text{Ba}_{1-x}\text{Sr}_x)\text{Y}_2\text{CuO}_5$ were obtained with a Rietveld pattern decomposition technique. These patterns represent ideal specimen patterns that

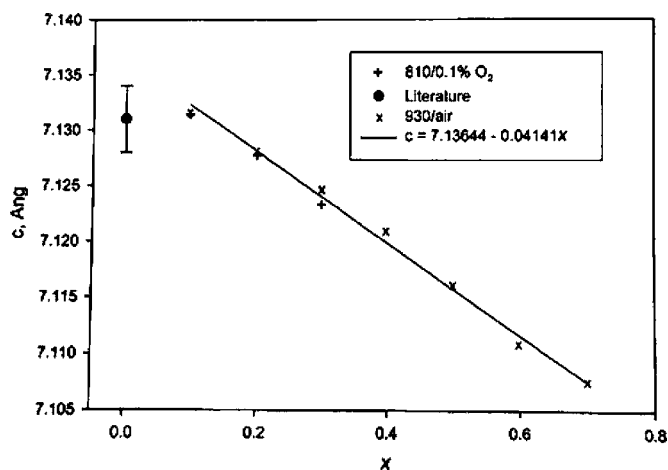


Figure 4. Variation of lattice parameter c versus composition (x) in $(\text{Ba}_{1-x}\text{Sr}_x)\text{Y}_2\text{CuO}_5$. The solid dot refers to the average literature c value for BaY_2CuO_5 (Wong-Ng *et al.*, 1989; Wong-Ng *et al.*, 1995; Watkins *et al.*, 1988; Michel and Raveau, 1982; Hazen *et al.*, 1987; Hsu *et al.*, 1996; Ross *et al.*, 1987; Fjellvag *et al.*, 1987; Sato and Nakada, 1989; Hunter *et al.*, 1989; Salinas-Sanchez *et al.*, 1992; Buttner and Maslen, 1993; Shaked *et al.*, 1993), with standard deviation (1 sigma) indicated.

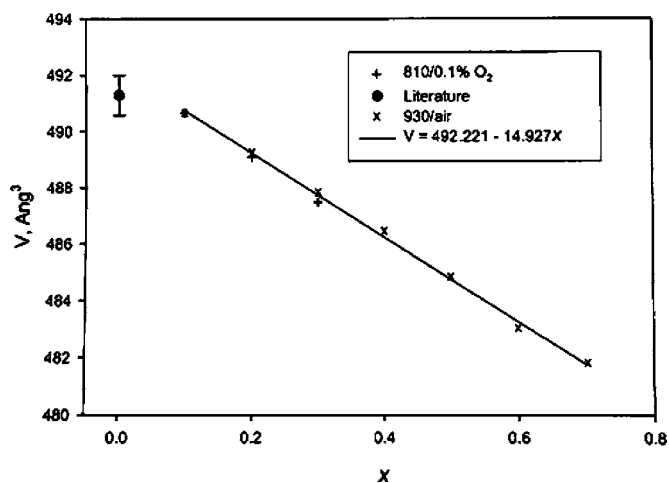


Figure 5. Variation of unit cell volume V versus composition (x) in $(\text{Ba}_{1-x}\text{Sr}_x)\text{Y}_2\text{CuO}_5$. The solid dot refers to the average literature V value for BaY_2CuO_5 (Wong-Ng *et al.*, 1989; Wong-Ng *et al.*, 1995; Watkins *et al.*, 1988; Michel and Raveau, 1982; Hazen *et al.*, 1987; Hsu *et al.*, 1996; Ross *et al.*, 1987; Fjellvag *et al.*, 1987; Sato and Nakada, 1989; Hunter *et al.*, 1989; Salinas-Sanchez *et al.*, 1992; Buttner and Maslen, 1993; Shaked *et al.*, 1993), with standard deviation (1 sigma) indicated.

have been corrected for systematic errors, both in d spacing and intensity. The reported peak positions are calculated from the refined lattice parameters, as they represent the best measure of the peak positions.

C. NPD experiment

To obtain detailed structural information and to confirm the Ba/Sr composition ratio, one member of the $(\text{Ba}_{1-x}\text{Sr}_x)\text{Y}_2\text{CuO}_5$ series with a nominal composition of $\text{Ba}_{0.5}\text{Sr}_{0.5}\text{Y}_2\text{CuO}_5$ was selected for the NPD study. NPD data were collected using the 32 detector BT-1 diffractometer with a Cu (311) monochromator ($\lambda = 1.5403 \text{ \AA}$) at the NIST Center for Neutron Research. Samples were loaded in a 0.5 in. diameter vanadium can. Measurement was made under ambient conditions. The 2θ angular scanning range was from 3° to 168° with steps of 0.05° . Structure refinement was performed using the program GSAS (Larson and von Dreele, 1985) and the initial structure parameters were taken from the report of BaY_2CuO_5 (Watkins *et al.*, 1988). The neutron scattering length for Ba, Sr, Y, Cu, and O are 0.525, 0.702, 0.775, 0.772, and $0.585 (\times 10^{-12} \text{ cm})$, respectively. The scale factor, background function parameters (high-order polynomials), profile parameters U , V , W , and asymmetry coefficient, lattice parameters, atomic coordinates, and mean square displacement factors were varied in the refinement. The mean square displacement factors of the same atom types were constrained to be equal in the calculation.

D. Differential thermal analysis/ thermogravimetric analysis (DTA/TGA)

Two selected samples, BaY_2CuO_5 and $\text{Ba}_{0.5}\text{Sr}_{0.5}\text{Y}_2\text{CuO}_5$ were used for DTA/TGA studies to determine the effect of atmosphere and annealing temperature on oxygen stoichiometry. For these studies, a Mettler TA1 thermoanalyzer equipped with Anatech control firmware and data acquisition software was employed. Sample masses of 55 mg to 60 mg,

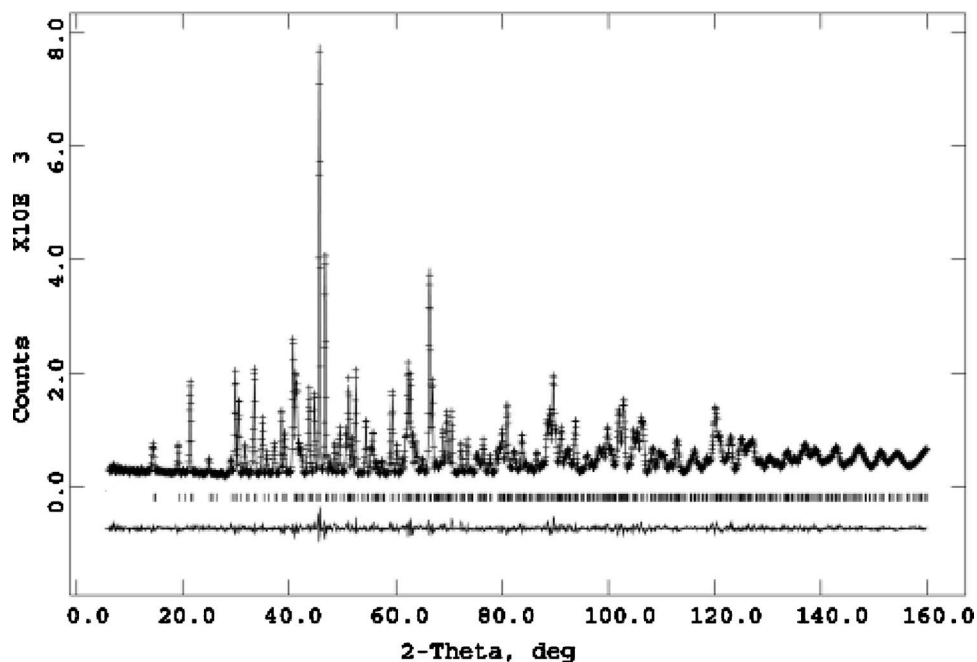


Figure 6. Observed (crosses) and calculated (solid line) NPD intensities pattern for $(\text{Ba}_{0.5}\text{Sr}_{0.5})\text{Y}_2\text{CuO}_5$ at 295 K. The differences are shown at the bottom of the figure. Vertical lines indicate the Bragg positions.

contained in MgO crucibles, were used. Gas of the desired composition, supplied from analyzed cylinders, was flowed continuously through the sample area at a rate of ≈ 70 ml/min. During the DTA experiments, temperature was ramped at $10^\circ\text{C}/\text{min}$. The DTA/TGA thermocouple was calibrated against the α/β quartz transition (571°C), and the melting points of NaCl (801°C) and Au (1064°C). DTA/TGA temperatures have an uncertainty of less than $\pm 5^\circ\text{C}$ (standard error of estimate).

III. RESULTS AND DISCUSSION

The results pertaining to the characterization of the $(\text{Ba}_{1-x}\text{Sr}_x)\text{Y}_2\text{CuO}_5$ solid solution are discussed in the following four areas: (1) Solid solution range for $(\text{Ba}_{1-x}\text{Sr}_x)\text{Y}_2\text{CuO}_5$; (2) Rietveld structural refinement of $(\text{Ba}_{0.5}\text{Sr}_{0.5})\text{Y}_2\text{CuO}_5$ using NPD data; (3) a comparison of the structure of the members in $(\text{Ba}_{1-x}\text{Sr}_x)\text{Y}_2\text{CuO}_5$; and (4) X-ray reference diffraction patterns for $(\text{Ba}_{1-x}\text{Sr}_x)\text{Y}_2\text{CuO}_5$.

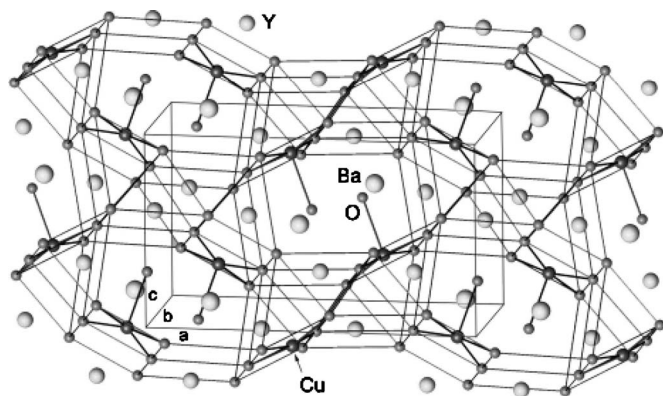


Figure 7. Perspective view of the $(\text{Ba}_{0.5}\text{Sr}_{0.5})\text{Y}_2\text{CuO}_5$ structure along the b axis, showing the isolated square pyramids of $[\text{CuO}_5]$ and the trigonal RO_7 prisms around the rare-earth atoms.

A. Solid solution range for $(\text{Ba}_{1-x}\text{Sr}_x)\text{Y}_2\text{CuO}_5$

A complete solid solution of $(\text{Ba}_{1-x}\text{Sr}_x)\text{Y}_2\text{CuO}_5$ was not obtained under both air and 100 Pa p_{O_2} . This result confirms the report by Roth *et al.* (1989) that the SrY_2CuO_5 phase is absent in the phase diagram of the $\text{SrO}-1/2\text{Y}_2\text{O}_3-\text{CuO}$ system. The XPD results showed that the single phase solid solution ranges for $(\text{Ba}_{1-x}\text{Sr}_x)\text{Y}_2\text{CuO}_5$ are $0 \leq x \leq 0.3$ and $0 \leq x \leq 0.7$ when the samples were prepared in 100 Pa p_{O_2} and in air, respectively. The X-ray diffraction patterns of the $(\text{Ba}_{1-x}\text{Sr}_x)\text{Y}_2\text{CuO}_5$ samples prepared in air are presented in Figure 1. A small amount of impurity phases, including Y_2O_3 , is discernible in the X-ray pattern of the $x=0.8$ sample. All single phase samples could be indexed by using the structure of the green phase, BaY_2CuO_5 , which has an orthorhombic Pnma space group.

The lattice parameters of $(\text{Ba}_{1-x}\text{Sr}_x)\text{Y}_2\text{CuO}_5$ obtained from powder XPD data are listed in Table I. As was expected, because the ionic radius of Sr^{2+} is smaller than that of Ba^{2+} (Shannon, 1976), the lattice parameters, a , b , and c , of the unit cell and volume, V , decrease as the amount of the Sr^{2+} (x) (Figures 2–5) increases. The linear dependence of the lattice parameters and the unit-cell volume on the content of the Sr^{2+} ion is expressed as following functions:

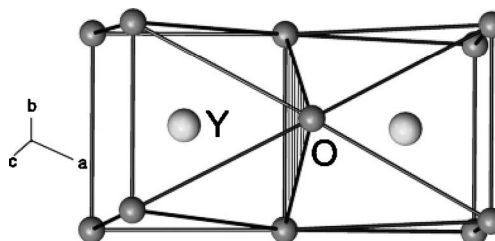


Figure 8. Coordination environments of Y_2O_{11} formed by two YO_7 groups found in the $(\text{Ba}_{0.5}\text{Sr}_{0.5})\text{Y}_2\text{CuO}_5$ structure.

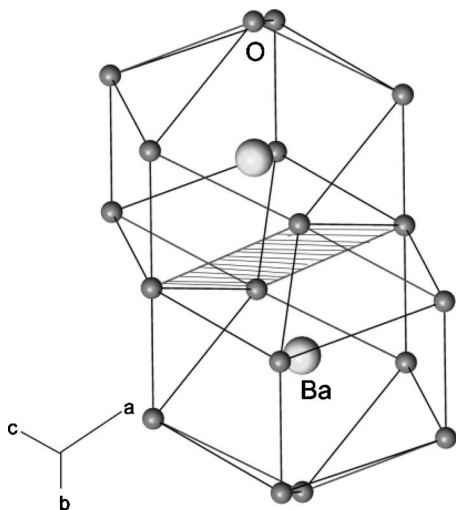


Figure 9. Coordination environments of $(\text{Ba}, \text{Sr})_2\text{O}_{18}$ formed by two $(\text{Ba}, \text{Sr})\text{O}_{11}$ units found in the $(\text{Ba}_{0.5}\text{Sr}_{0.5})\text{Y}_2\text{CuO}_5$ structure.

$$a = 12.18412 - 0.15684x,$$

$$b = 5.666090 - 0.06695x,$$

$$c = 7.13644 - 0.04141x,$$

$$V = 492.221 - 14.927x.$$

Because the solid solution range is different for the two series of samples, it is likely the result of them being annealed at two different temperatures. Refinement results using neutron diffraction data (discussed below) did not indicate any oxygen-deficient sites. Furthermore, DTA/TGA results suggest that oxidation/reduction was not involved in this series of samples. For example, the DTA/TGA data for the BaY_2CuO_5 sample did not show any measurable oxygen loss as the sample was heated under $p_{\text{O}_2}=100$ Pa until the sample melted at ≈ 1192 °C. Similarly, as the $\text{Ba}_{0.5}\text{Sr}_{0.5}\text{Y}_2\text{CuO}_5$ sample was annealed at 600 °C, at $p_{\text{O}_2}=100$ Pa, then annealed at 810 °C, at $p_{\text{O}_2}=100$ Pa, there was no thermogravimetric indication of a change in oxygen stoichiometry. The same $\text{Ba}_{0.5}\text{Sr}_{0.5}\text{Y}_2\text{CuO}_5$ sample was annealed further at 600 °C in 100% O_2 for 10 h, followed by annealing at 810 °C at $p_{\text{O}_2}=100$ Pa for 10 h; again there was no indication of a change in oxygen stoichiometry.

B. Structural refinement of $(\text{Ba}_{0.5}\text{Sr}_{0.5})\text{Y}_2\text{CuO}_5$ (NPD)

The refinement result of $(\text{Ba}_{0.5}\text{Sr}_{0.5})\text{Y}_2\text{CuO}_5$ gives the ratio of 0.501 (27)/0.499(27) for Ba/Sr, which agrees very well with the nominal composition. Refinement of oxygen content yielded the occupancies of 1.007(8), 0.984(9), and 1.008(8) for O1, O2, and O3, respectively. Compositions for the other $(\text{Ba}_{1-x}\text{Sr}_x)\text{Y}_2\text{CuO}_5$ compounds were, therefore, fixed at their nominal compositions in further structural analyses. Figure 6 shows the observed and calculated NPD pattern for $(\text{Ba}_{0.5}\text{Sr}_{0.5})\text{Y}_2\text{CuO}_5$ at room temperature.

Figure 7 presents a perspective view of the structure of $(\text{Ba}_{0.5}\text{Sr}_{0.5})\text{Y}_2\text{CuO}_5$ along the b axis. $(\text{Ba}_{0.5}\text{Sr}_{0.5})\text{Y}_2\text{CuO}_5$ is confirmed to be isostructural to the green phase BaR_2CuO_5

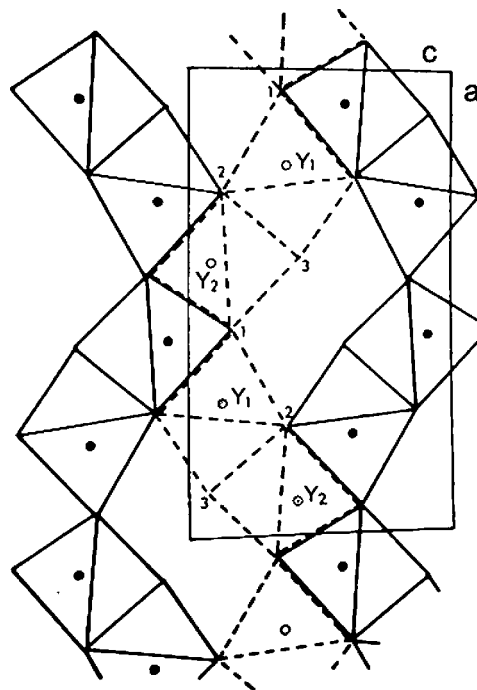


Figure 10. Projection of the structure of $(\text{Ba}_{0.5}\text{Sr}_{0.5})\text{Y}_2\text{CuO}_5$ at $y=1/4$ (broken line) and $y=3/4$ (solid line).

analogues (R=lanthanides) (Wong-Ng *et al.*, 1989; Wong-Ng *et al.*, 1995; Watkins *et al.*, 1988; Michel and Raveau, 1982; Hazen *et al.*, 1987; Hsu *et al.*, 1996; Ross *et al.*, 1987; Fjellvag *et al.*, 1987; Sato and Nakada, 1989; Hunter *et al.*, 1989; Salinas-Sanchez *et al.*, 1992; Buttner and Maslen, 1993; Shaked *et al.*, 1993). The general structure of $(\text{Ba}_{0.5}\text{Sr}_{0.5})\text{Y}_2\text{CuO}_5$ consists of a three-dimensional network of interconnected $[\text{YO}_7]$, $[(\text{Ba}, \text{Sr})\text{O}_{11}]$, and $[\text{CuO}_5]$ polyhedra. The copper ions are situated in distorted “square” pyramids $[\text{CuO}_5]$. The $[\text{Y}_2\text{O}_{11}]$ groups are formed from two monocapped trigonal $[\text{YO}_7]$ prisms sharing a triangular face (Figure 8). The $(\text{Ba}, \text{Sr})^{2+}$ ions are found to reside in distorted 11-fold coordinated cages (Figure 9).

All cations were found to be located in layers along the y axis, the shortest axis. Consecutive layers are displaced by the n glide, and the $[\text{YO}_7]$ prisms are stacked parallel to each other with shared trigonal faces (Figure 7). In Figure 10, the projection of the Y_2O_{11} blocks at $y=1/4$ is shown as solid lines and the upper layer at $y=3/4$ is represented as dotted lines. These $[\text{YO}_7]$ prisms can also be viewed as sharing edges to form wavelike chains parallel to the long x axis that are crosslinked by the Cu and Ba ions.

C. Comparison of the structure of the $(\text{Ba}_{1-x}\text{Sr}_x)\text{Y}_2\text{CuO}_5$ members

Results of structural refinement for $(\text{Ba}_{1-x}\text{Sr}_x)\text{Y}_2\text{CuO}_5$ using the X-ray data with the GSAS program suite are reported in Table I. Table II cites the Rietveld refinement results for $(\text{Ba}_{1-x}\text{Sr}_x)\text{Y}_2\text{CuO}_5$. The corresponding refined structural parameter that include the final refined positional and thermal parameters are given in Table III. As expected, the values of the final atomic coordinates for each atom are

TABLE II. Rietveld refinement results for $(\text{Ba}_{1-x}\text{Sr}_x)\text{Y}_2\text{CuO}_5$. Readers are referred to Larson and von Dreele (1985) for the definitions for the symbols in this table.

x	0.10		0.20		0.30		0.40	0.50	0.60	0.70
	810 °C		810 °C		810 °C		810 °C	810 °C	810 °C	810 °C
	100 Pa	930 °C	100 Pa	930 °C	100 Pa	930 °C				
Prep. condition	p_{O_2}	air	p_{O_2}	air	p_{O_2}	air	air	air	air	air
wRp	0.0404	0.0388	0.0405	0.0666	0.0674	0.0493	0.0421	0.0583	0.0541	0.0541
Rp	0.0393	0.0302	0.0308	0.0520	0.0529	0.0379	0.0328	0.0456	0.0417	0.0419
χ^2	2.091	1.974	2.154	1.206	1.496	1.375	2.419	1.896	1.720	1.834
$R(F)$	0.0288	0.0206	0.0244	0.0347	0.0428	0.02240	0.0318	0.0333	0.0366	0.0323
$R(F^2)$	0.0429	0.0333	0.0343	0.0523	0.0666	0.0356	0.0544	0.0535	0.0540	0.0506
ΔF_{\pm}^+	1.25	1.21	1.03	2.11	2.08	1.13	2.08	1.79	1.87	1.46
	-1.55	-0.92	-1.26	-2.08	-1.87	-1.26	-1.36	-1.69	-1.69	-1.83
U	0.288	26.5(4)	0.288	0.288	0.288	0.336	0.336	0.336	0.114	16.41
X	6.27(1)	5.92(2)	6.17(1)	5.03(2)	7.25(3)	3.44(5)	2.526	6.22(7)	7.12(4)	4.51(8)
Y	2.103	2.103	2.103	2.103	2.103	$S(hkl)$	$S(hkl)$	$S(hkl)$	$S(hkl)$	$S(hkl)$

rather similar in all members of $(\text{Ba}_{1-x}\text{Sr}_x)\text{Y}_2\text{CuO}_5$, as compared to those for BaY_2CuO_5 .

Selected interatomic distances for $(\text{Ba}_{1-x}\text{Sr}_x)\text{Y}_2\text{CuO}_5$ are listed in Table IV. Because the ionic radius of the Sr^{2+} ion is substantially smaller than that of the Ba^{2+} ion (Shannon, 1976), the change in the (Ba, Sr)–O bond length with composition [i.e., with the “x” value in $(\text{Ba}_{1-x}\text{Sr}_x)\text{Y}_2\text{CuO}_5$] is more apparent than those of other metal-oxygen bond distances. It is this notable shortening of the (Ba, Sr)–O bonds that is primarily responsible for the apparent decrease of the lattice parameters with increasing Sr^{2+} content (x). Within

the $[(\text{Ba}, \text{Sr})\text{O}_{11}]$ group, the (Ba, Sr)–O bond distances are between 2.493 Å and 3.253 Å, giving rise to a much distorted polyhedron.

The bond valence sum values, V_b , for Ba, Y, and Cu were calculated using the Brown-Altarmatt empirical expression (Brese and O’Keeffe, 1991; Brown and Altarmatt, 1985), and the results are listed in Table V. The V_b of an atom i is defined as the sum of the bond valences v_{ij} of all the bonds from atoms i to atoms j . The most commonly adopted empirical expression for the bond valence v_{ij} as a function of the interatomic distance d_{ij} is

TABLE III. Refined structural parameters of the orthorhombic $(\text{Ba}_{1-x}\text{Sr}_x)\text{Y}_2\text{CuO}_5$ compounds ($y=1/4$ for Ba/Sr, Y, Cu and O3).

x	0.10		0.20		0.30		0.40	0.50	0.60	0.70
	810 °C		810 °C		810 °C		810 °C	810 °C	810 °C	810 °C
	100 Pa	930 °C	100 Pa	930 °C	100 Pa	930 °C				
Prep. condition	p_{O_2}	air	p_{O_2}	air	p_{O_2}	air	air	air	air	air
Ba/Sr, x	0.9055(0)	0.9054(0)	0.9058(0)	0.9057(0)	0.9061(1)	0.9063(0)	0.9072(0)	0.9078(1)	0.9085(1)	0.9090(1)
Z	0.9302(0)	0.9300(0)	0.9300(0)	0.9295(1)	0.9299(1)	0.9296(1)	0.9288(1)	0.9289(1)	0.9281(1)	0.9280(1)
U_{iso}	0.58(2)	0.39(2)	0.43(2)	0.70(3)	0.36(3)	0.70(2)	0.30	0.30	0.76(4)	0.95(4)
Y1, x	0.2881(0)	0.2883(0)	0.2881(0)	0.2883(1)	0.2882(1)	0.2882(0)	0.2881(1)	0.2878(1)	0.2877(1)	0.2876(1)
Z	0.1161(1)	0.1164(1)	0.1162(1)	0.1163(2)	0.1154(2)	0.1159(1)	0.1159(1)	0.1157(2)	0.1154(1)	0.1160(1)
U_{iso}	0.22(1)	0.06(1)	0.05(1)	0.28(2)	0.05(2)	0.25(1)	0.20	0.20	0.01(2)	0.28(2)
Y2, x	0.0740(0)	0.0741(0)	0.0739(0)	0.0739(1)	0.0735(1)	0.0742(0)	0.0737(1)	0.0739(1)	0.0739(1)	0.0738(1)
Z	0.3957(1)	0.3958(1)	0.3955(1)	0.3953(1)	0.3950(2)	0.3949(1)	0.3952(1)	0.3951(1)	0.3946(1)	0.3949(1)
Cu, x	0.6594(1)	0.6593(1)	0.6595(1)	0.6598(2)	0.6598(2)	0.6597(1)	0.6599(1)	0.6605(2)	0.6606(1)	0.6606(1)
Z	0.7135(1)	0.7136(1)	0.7138(1)	0.7131(2)	0.7140(3)	0.7135(2)	0.7145(2)	0.7139(3)	0.7139(2)	0.7141(2)
U_{iso}	0.42(4)	0.26(4)	0.28(4)	0.50(6)	0.21(7)	0.50(5)	0.20	0.20	0.33(6)	0.48(6)
O1, x	0.4328(3)	0.4333(3)	0.4330(3)	0.4327(4)	0.4312(4)	0.4320(3)	0.4330(4)	0.4327(5)	0.4323(4)	0.4326(4)
y	-0.0065(7)	-0.0080(6)	-0.0065(7)	-0.0088(8)	-0.0091(8)	-0.0074(7)	-0.0075(8)	-0.0080(9)	-0.0088(8)	-0.0074(8)
Z	0.1646(5)	0.1649(4)	0.1646(5)	0.1640(6)	0.1618(7)	0.1642(5)	0.1662(5)	0.1662(7)	0.1648(6)	0.1645(5)
U_{iso}	1.0	1.0	1.0	1.0	1.0	1.0	1.0	1.0	1.0	1.0
O2, x	0.2252(3)	0.2254(2)	0.2252(3)	0.2257(4)	0.2251(4)	0.2257(3)	0.2240(4)	0.2246(4)	0.2241(4)	0.2246(4)
y	0.5050(7)	0.5058(7)	0.5044(7)	0.5059(9)	0.5055(10)	0.5064(8)	0.5020(9)	0.5054(10)	0.5058(9)	0.5056(8)
Z	0.3532(6)	0.3531(6)	0.3522(6)	0.3523(7)	0.3491(8)	0.3528(6)	0.3527(7)	0.3510(8)	0.3485(7)	0.3482(7)
U_{iso}	1.0	1.0	1.0	1.0	1.0	1.0	1.0	1.0	1.0	1.0
O3, x	0.0988(4)	0.0983(4)	0.0983(4)	0.0994(6)	0.0982(6)	0.0979(5)	0.0957(6)	0.0977(7)	0.0968(6)	0.0962(5)
Z	0.0774(7)	0.0779(7)	0.0765(8)	0.0764(9)	0.0760(10)	0.0759(8)	0.0753(9)	0.0728(10)	0.0752(9)	0.0750(8)
U_{iso}	1.0	1.0	1.0	1.0	1.0	1.0	1.0	1.0	1.0	1.0

TABLE IV. Selected bond distances (Å) in orthorhombic (Ba_{1-x}Sr_x)Y₂CuO₅ compounds.

x	0.10		0.20		0.30		0.40	0.50	0.60	0.70
	810 °C 100 Pa pO ₂	930 °C air	810 °C 100 Pa pO ₂	930 °C air	810 °C 100 Pa pO ₂	930 °C air				
Ba/Sr										
-O1 × 2	3.058(4)	3.049(4)	3.050(4)	3.049(5)	3.064(5)	3.049(4)	3.019(5)	3.012(6)	3.007(5)	3.003(5)
-O1 × 2	3.250(4)	3.253(3)	3.249(4)	3.261(5)	3.268(5)	3.253(4)	3.243(4)	3.241(5)	3.252(4)	3.249(4)
-O2 × 2	2.922(4)	2.918(4)	2.916(4)	2.913(7)	2.896(7)	2.917(5)	2.916(5)	2.904(7)	2.884(6)	2.889(6)
-O2 × 2	3.045(4)	3.046(4)	3.047(4)	3.048(7)	3.062(7)	3.050(5)	3.061(5)	3.073(7)	3.091(6)	3.090(5)
-O3 × 1	2.576(6)	2.574(6)	2.562(6)	2.576(7)	2.552(8)	2.549(6)	2.512(8)	2.516(9)	2.505(7)	2.490(7)
-O3 × 2	2.827(0)	2.827(0)	2.824(0)	2.824(0)	2.820(0)	2.821(0)	2.817(0)	2.814(0)	2.810(0)	2.807(0)
Y1										
-O1 × 2	2.307(4)	2.315(4)	2.306(4)	2.308(5)	2.292(6)	2.297(4)	2.306(5)	2.305(6)	2.301(5)	2.295(5)
-O1 × 2	2.350(4)	2.350(4)	2.340(4)	2.345(4)	2.331(5)	2.349(4)	2.337(5)	2.336(5)	2.324(5)	2.316(4)
-O2 × 2	2.337(4)	2.337(4)	2.343(4)	2.339(4)	2.331(5)	2.330(4)	2.343(5)	2.338(5)	2.347(4)	2.351(4)
-O3 × 1	2.320(6)	2.328(6)	2.323(6)	2.314(7)	2.324(8)	2.327(6)	2.351(7)	2.322(8)	2.325(7)	2.330(7)
Y2										
-O1 × 2	2.361(3)	2.358(3)	2.361(3)	2.351(4)	2.337(5)	2.358(4)	2.366(4)	2.362(5)	2.352(4)	2.352(4)
-O2 × 2	2.289(4)	2.292(4)	2.283(4)	2.294(4)	2.298(4)	2.294(4)	2.282(5)	2.286(5)	2.286(4)	2.275(4)
-O2 × 2	2.357(4)	2.360(4)	2.354(4)	2.363(4)	2.359(4)	2.359(4)	2.329(4)	2.343(5)	2.338(4)	2.342(4)
-O3 × 1	2.290(5)	2.286(5)	2.293(5)	2.295(6)	2.292(7)	2.291(5)	2.294(6)	2.312(7)	2.289(6)	2.290(6)
Cu										
-O1 × 2	1.977(4)	1.973(3)	1.976(4)	1.972(4)	1.962(4)	1.968(3)	1.964(4)	1.963(4)	1.960(4)	1.966(4)
-O2 × 2	2.028(4)	2.024(3)	2.026(4)	2.013(4)	2.013(4)	2.011(3)	2.040(4)	2.011(4)	2.005(4)	2.000(4)
-O3 × 1	2.201(5)	2.208(5)	2.199(5)	2.190(6)	2.197(6)	2.194(5)	2.206(6)	2.178(7)	2.196(6)	2.197(6)

$$v_{ij} = \exp[(R_0 - d_{ij})/B].$$

The parameter, B , is commonly taken to be a “universal” constant equal to 0.37 Å. The values of the reference distance R_0 for Ba–O, Cu–O, and Y–O are 2.285, 1.679, and 2.019 Å, respectively (Brese and O’Keeffe, 1991; Brown and Altermatt, 1985). In Table V, note that the V_b values for Cu, and Y in all (Ba_{1-x}Sr_x)Y₂CuO₅ solid solution members, are very close to the ideal values of 2 and 3, respectively. While the V_b values for the (Ba, Sr) site are all less than the ideal value of 2 (underbonding, tensile stress, or atom in a oversized cage), they decrease from 1.862 ($x=0.1$) to a small value of 1.573 ($x=0.7$).

D. X-ray reference powder diffraction patterns for (Ba_{1-x}Sr_x)Y₂CuO₅

The X-ray powder reference patterns for (Ba_{0.3}Sr_{0.7})Y₂CuO₅ (Table VI) and (Ba_{0.7}Sr_{0.3})Y₂CuO₅ (Table VII) have been prepared and submitted to the International Centre for Diffraction Data (ICDD) to be included

in the PDF. In these tables, the symbols M and $+$ refer to peaks containing contributions from two and more than two reflections, respectively. The symbol * indicates the particular peak that has the strongest intensity of the entire pattern and is designated a value of “999.” The intensity values reported are integrated intensities rather than peak heights.

IV. SUMMARY

The green phase solid solution series, (Ba_{1-x}Sr_x)Y₂CuO₅, was investigated by X-ray and neutron Rietveld refinements. All single phase samples could be indexed using an orthorhombic cell with the space group Pnma (No. 64). Lattice parameters, a , b , and c , and the cell volume, V , decrease linearly with the increase of the content (x) of Sr. The general structure of (Ba_{1-x}Sr_x)Y₂CuO₅ consists of [YO₇], [(Ba, Sr)O₁₁], and [CuO₅] polyhedra. The copper ions are located inside distorted square pyramids [CuO₅]. These pyramids are connected by [Y₂O₁₁] groups that are comprised of two monocapped [YO₇] trigonal prisms sharing

 TABLE V. Bond valence sum (V_b) in (Ba_{1-x}Sr_x)Y₂CuO₅. (Brese and O’Keeffe, 1991; Brown and Altermatt, 1985).

	0.10		0.20		0.30		0.40	0.50	0.60	0.70
	100 Pa pO ₂	air	100 Pa pO ₂	air	100 Pa pO ₂	air	air	air	air	air
Ba/Sr	1.853	1.862	1.810	1.796	1.750	1.757	1.739	1.675	1.631	1.573
Y1	3.027	2.999	3.034	3.037	3.073	3.058	3.001	3.055	3.075	3.094
Y1	3.042	3.037	3.060	3.034	3.066	3.033	3.138	3.064	3.117	3.132
Cu	1.917	1.935	1.924	1.969	1.987	1.979	1.913	2.002	2.004	2.005

TABLE VI. X-ray reference pattern for $(\text{Ba}_{0.3}\text{Sr}_{0.7})\text{Y}_2\text{CuO}_5$, Pnma (No. 62), $a=12.07546(11)$ Å, $b=5.61419(5)$ Å, and $c=7.10741(6)$ Å. The symbol “ d ” refers to d -spacing values, I refers to integrated intensity value (scaled according to the maximum value of 999); the symbol* indicates the strongest peak); the hkl values are the Miller indexes; M and + refer to peaks containing contributions from two and more than two reflections, respectively.

$d[\text{Å}]$	I	h	k	l	$d[\text{Å}]$	I	h	k	l	$d[\text{Å}]$	I	h	k	l
4.4056	6	0	1	1	4.1114	7	2	1	0	3.4091	41	1	0	2
3.0626	68	2	0	2	3.0189	37	4	0	0	2.9716	999*	3	1	1
2.9140	701	1	1	2	2.8071	521	0	2	0	2.7786	216	4	0	1
2.6886	161	2	1	2	2.6589	26	4	1	0	2.5519	17	1	2	1
2.4903	96	4	1	1	2.4068	81	3	1	2	2.3248	30	1	0	3
2.2867	79	5	0	1	2.2054	187	2	0	3	2.2028	29	0	2	2
2.1828	88	0	1	3	2.1670	94	1	2	2	2.1479	62	1	1	3
2.1289	11	4	1	2	2.1178	37	5	1	1	2.0694	34	2	2	2
2.0557	56	4	2	0	2.0527	45	2	1	3	2.0126	82	6	0	0
1.9748	431	4	2	1	1.9364	6	6	0	1	1.9324	119	3	2	2
1.9188	22	3	1	3	1.8945	10	6	1	0	1.8819	6	5	1	2
1.8637	111	4	0	3	1.8306	41	6	1	1	1.7769	59	0	0	4
1.7729	60	5	2	1	1.7688	9	4	1	3	1.7579	29	1	0	4
1.7512	40	6	0	2	1.7342	158	2	2	3	1.6771	68	1	1	4M
1.6771	68	7	0	1M	1.6506	177	3	3	1	1.6405	130	1	3	2
1.6356	23	6	2	0	1.6063	25	7	1	1	1.5969	30	2	3	2
1.5940	8	6	2	1	1.5526	154	4	2	3M	1.5526	154	4	3	1M
1.5338	12	6	0	3	1.5313	21	3	3	2	1.5094	16	8	0	0
1.5014	27	0	2	4	1.4958	130	7	1	2	1.4899	26	1	2	4
1.4858	69	6	2	2	1.4772	89	4	1	4M	1.4772	89	8	0	1M
1.4685	21	0	3	3	1.4577	63	1	3	3M	1.4577	63	8	1	0M
1.4482	10	5	3	1	1.4393	10	7	2	1	1.4272	18	8	1	1M
1.4272	18	2	3	3M	1.4067	18	3	2	4	1.4036	100	0	4	0
1.3946	33	7	0	3	1.3869	24	5	1	4	1.3836	5	2	0	5
1.3796	5	3	3	3	1.3780	24	0	1	5	1.3582	14	7	2	2
1.3459	34	6	2	3M	1.3459	34	6	3	1M	1.3320	29	6	0	4
1.3294	12	8	2	0	1.3068	9	8	2	1	1.3037	83	3	1	5
1.2979	6	1	4	2	1.2835	17	9	1	1	1.2813	12	1	3	4
1.2612	10	1	2	5	1.2528	41	4	4	1	1.2488	21	7	2	3M
1.2488	21	7	3	1M	1.2415	12	8	1	3	1.2250	7	5	0	5
1.2095	9	3	2	5	1.2087	38	7	1	4	1.2034	23	6	2	4
1.2016	6	1	4	3	1.1962	17	5	4	1	1.1946	67	7	3	2
1.1846	88	0	0	6+	1.1806	13	10	1	0	1.1749	20	8	3	0
1.1512	19	6	4	0	1.1504	5	8	0	4	1.1433	6	10	0	2
1.1366	26	5	3	4M	1.1366	26	3	0	6M	1.1320	12	0	3	5
1.1228	9	5	2	5	1.1212	38	4	4	3	1.1093	8	10	2	0
1.1014	22	0	4	4	1.0968	10	1	4	4	1.0960	16	10	2	1
1.0952	15	6	4	2	1.0914	30	0	2	6	1.0897	46	3	3	5
1.0869	7	1	2	6	1.0849	6	11	0	1	1.0779	16	9	2	3M
1.0779	16	9	3	1M	1.0760	37	7	4	1M	1.0760	37	10	0	3M
1.0692	44	3	5	1	1.0665	28	1	5	2	1.0652	14	11	1	1
1.0645	7	8	2	4	1.0589	9	10	2	2	1.0533	32	3	2	6
1.0526	8	8	3	3	1.0489	13	11	0	2	1.0411	6	4	5	1
1.0355	6	6	4	3	1.0348	13	8	0	5M	1.0348	13	3	5	2M
1.0324	19	7	3	4	1.0279	8	8	4	0	1.0218	9	7	2	5
1.0209	5	6	0	6	1.0173	5	8	4	1	1.0147	16	10	3	0M
1.0147	16	0	5	3M	1.0119	13	11	2	1M	1.0119	13	1	0	7M
1.0111	5	1	5	3	1.0046	44	10	2	3	1.9991	13	0	1	7
0.9893	24	7	4	3	0.9833	12	10	1	4	0.9825	38	11	2	2
0.9810	7	12	1	1	0.9710	25	6	5	1M	0.9710	25	8	2	5M
0.9694	5	3	4	5	0.9662	24	6	4	4	0.9622	41	4	0	7M
0.9622	41	7	1	6M	0.9594	23	6	2	6	0.9518	8	1	2	7
0.9463	8	1	5	4	0.9410	10	10	2	4	0.9386	11	11	3	1
0.9357	21	0	6	0	0.9329	5	7	5	1	0.9290	7	3	2	7
0.9233	8	5	1	7	0.9229	8	5	4	5	0.9223	5	7	2	6
0.9213	5	11	1	4	0.9193	5	8	1	6	0.9104	19	4	2	7
0.9097	39	7	5	2	0.9089	10	13	1	1	0.9054	35	4	5	4M
0.9054	35	0	4	6M	0.9023	6	1	6	2	0.9009	12	8	5	0
0.8949	9	6	1	7	0.8925	13	0	3	7	0.8897	10	8	4	4
0.8874	18	13	1	2	0.8867	46	4	6	1M	0.8867	46	10	4	2M
0.8844	7	8	2	6	0.8833	31	5	5	4M	0.8833	31	3	4	6M
0.8828	12	3	6	2	0.8811	19	10	3	4M	0.8811	19	0	5	5M
0.8795	7	12	3	1	0.8752	16	1	1	8	0.8673	11	3	0	8M
0.8673	11	4	4	6M	0.8657	29	7	3	6	0.8645	17	7	1	7M
0.8645	17	7	4	5M	0.8625	9	14	0	0	0.8614	24	2	6	3
0.8607	43	3	5	5	0.8586	40	11	1	5	0.8584	11	11	4	1

TABLE VII. X-ray reference pattern for Ba_{0.7}Sr_{3.0}CuO₅, Pnma (No. 62), $a=12.13823(7)$ Å, $b=5.64148(3)$ Å, and $c=7.12494(3)$ Å. The symbol “ d ” refers to d -spacing values, “ I ” refers to integrated intensity value (scaled according to the maximum value of 999; the symbol $\bar{1}$ indicates the strongest peak); the hkl values are the Miller indexes; M and + refer to peaks containing contributions from two and more than two reflections, respectively.

$d[\text{Å}]$	I	h	k	l	$d[\text{Å}]$	I	h	k	l	$d[\text{Å}]$	I	h	k	l
4.1320	4	2	1	0	3.5625	6	0	0	2	3.4183	48	1	0	2
3.0723	48	2	0	2	3.0346	54	4	0	0	2.9854	999 [*]	3	1	1
2.9235	692	1	1	2	2.8207	484	0	2	0	2.7919	197	4	0	1
2.6981	181	2	2	2	2.6725	18	4	1	0	2.5635	32	1	2	1
2.5022	96	4	1	1	2.4161	84	3	1	2	2.4075	8	2	2	1
2.3308	32	1	0	3	2.2979	91	5	0	1	2.2116	223	2	0	3M
2.2116	223	0	2	2M	2.1889	58	0	1	3	2.1756	96	1	2	2
2.1542	60	1	1	3	2.1378	5	4	1	2	2.1282	30	5	1	1
2.0778	30	2	2	2	2.0660	68	4	2	0	2.0591	42	2	1	3
2.0230	81	6	0	0	1.9843	369	4	2	1	1.9461	7	6	0	1
1.9405	83	3	2	2	1.9252	15	3	1	3	1.8902	10	5	1	2
1.8703	97	4	0	3	1.8397	31	6	1	1	1.7814	121	5	2	1M
1.7814	121	0	0	4M	1.7753	15	4	1	3	1.7624	31	1	0	4
1.7592	41	6	0	2	1.7405	162	2	2	3	1.6849	27	7	0	1
1.6822	43	1	1	4	1.6585	173	3	3	1	1.6476	126	1	3	2
1.6439	25	6	2	0	1.6257	6	5	1	3	1.6144	36	7	1	1
1.6039	29	2	3	2	1.6019	8	6	2	1	1.5589	152	4	2	3+
1.5400	14	6	0	3	1.5392	21	3	3	2	1.5173	12	8	0	0
1.5061	22	0	2	4	1.5028	109	7	1	2	1.4946	29	1	2	4
1.4927	68	6	2	2	1.4857	6	6	1	3	1.4840	12	8	0	1
1.4822	70	4	1	4	1.4743	14	0	3	3	1.4652	49	8	1	0
1.4636	16	1	3	3	1.4553	8	5	3	1	1.4465	8	7	2	1
1.4352	6	8	1	1	1.4326	12	2	3	3	1.4106	115	3	2	4M
1.4106	115	0	4	0M	1.4005	31	7	0	3	1.3917	31	5	1	4
1.3873	7	2	0	5	1.3816	26	0	1	5	1.3646	17	7	2	2
1.3519	31	6	3	1M	1.3519	31	6	2	3M	1.3367	34	6	0	4M
1.3367	34	8	2	0M	1.3261	7	4	3	3	1.3133	8	8	2	1
1.3075	74	3	1	5	1.3038	7	1	4	2	1.2901	18	9	1	1
1.2859	16	1	3	4	1.2790	5	4	4	0	1.2650	8	1	2	5
1.2589	34	4	4	1	1.2547	25	7	3	1M	1.2547	25	7	2	3M
1.2470	13	8	1	3	1.2449	7	2	2	5	1.2289	7	5	0	5
1.2135	43	7	1	4+	1.2081	19	6	2	4	1.2067	6	1	4	3
1.2020	20	5	4	1	1.2003	56	7	3	2	1.1894	75	4	3	4M
1.1894	75	2	4	3M	1.1875	9	0	0	6	1.1867	12	10	1	0
1.1808	22	8	3	0	1.1570	19	6	4	0	1.1490	8	10	0	2
1.1414	15	5	3	4	1.1409	5	6	1	5	1.1394	14	3	0	6
1.1357	14	0	3	5	1.1262	45	5	2	5M	1.1262	45	4	4	3M
1.1150	11	10	2	0	1.1057	18	0	4	4	1.1014	23	10	2	1M
1.1014	23	1	4	4M	1.1004	15	6	4	2	1.0945	29	0	2	6
1.0935	43	3	3	5	1.0903	13	11	0	1M	1.0903	13	1	2	6M
1.0831	2	9	3	1M	1.0831	17	9	2	3M	1.0815	11	7	4	1
1.0808	17	10	0	3	1.0744	45	3	5	1	1.0714	28	1	5	2
1.0707	9	11	1	1	1.0689	6	8	2	4	1.0641	11	10	2	2
1.0591	7	2	5	2	1.0574	9	8	3	3	1.0564	39	3	2	6M
1.0564	39	9	1	4M	1.0541	15	11	0	2	1.0461	6	4	5	1
1.0399	13	6	4	3M	1.0399	13	3	5	2M	1.0387	8	8	0	5
1.0367	18	7	3	4	1.0330	6	8	4	0	1.0256	7	7	2	5
1.0241	6	6	0	6	1.0223	5	8	4	1	1.0198	7	10	3	0
1.0171	7	11	2	1	1.0143	7	1	0	7	1.0093	35	10	2	3
1.0017	14	0	1	7	0.9956	6	12	1	0	0.9938	21	7	4	3
0.9890	6	2	4	5	0.9874	49	10	1	4M	0.9874	49	11	2	2M
0.9861	6	12	1	1	0.9747	20	8	2	5	0.9703	20	6	4	4
0.9652	32	7	1	6M	0.9652	32	4	0	7M	0.9626	23	6	2	6
0.9545	9	1	2	7	0.9502	9	1	5	4	0.9451	9	10	2	4
0.9433	7	11	3	1	0.9403	21	0	6	0	0.9375	7	7	5	1
0.9334	6	9	3	4	0.9317	8	3	2	7	0.9263	13	5	4	5M
0.9263	13	5	1	7M	0.9254	14	7	2	6M	0.9254	14	11	1	4M
0.9226	7	8	1	6	0.9200	6	10	4	0	0.9141	32	7	5	2
0.9136	14	13	1	1	0.9131	15	4	2	7	0.9119	6	10	1	5
0.9094	21	4	5	4	0.9084	12	0	4	6	0.9066	6	1	6	2
0.9054	14	8	5	0	0.8977	8	6	1	7	0.8951	14	0	3	7
0.8936	8	8	4	4	0.8919	12	13	1	2	0.8910	48	4	6	1+
0.8871	20	5	5	4M	0.8871	20	3	6	2M	0.8863	22	3	4	6
0.8848	19	10	3	4M	0.8848	19	0	5	5M	0.8839	6	12	3	1
0.8774	15	1	1	8	0.8703	21	5	6	1+	0.8689	22	7	3	6
0.8678	8	7	4	5	0.8673	15	7	1	7M	0.8673	15	14	0	0M

a triangular face. The Ba^{2+} atoms are found to reside in distorted 11-fold coordinated cages. Unlike the superconductor phase, $\text{Ba}_2\text{YCu}_3\text{O}_{6+x}$, there is no significant variation in the oxygen content in $(\text{Ba}_{1-x}\text{Sr}_x)\text{Y}_2\text{CuO}_5$.

ACKNOWLEDGMENTS

The authors acknowledge the partial financial support from International Centre for Diffraction Data (ICDD) and the U.S. Department of Energy (DOE).

- Arendt, P. N. and Foltyn, S. R. (2004). "Biaxially textured IBAD-MgO templates for YBCO-coated conductors," *MRS Bull.* **29**, 543–550.
- Aytug, T., Goyal, A., Rutter, N., Paranthaman, M., Thompson, J. R., Zhai, H. Y., and Christen, D. K. (2003). "High- T_c $\text{YBa}_2\text{Cu}_3\text{O}_7$ coatings on LaMnO_3 -buffered biaxially textured Cu tapes for coated conductor applications," *J. Mater. Res.* **18**, 872–877.
- Balachandran, U. and Chudzik, M. P. (2002). "Method for preparing high-temperature superconductor," U.S. Patent No. 6,361,598 (March 26, 2002).
- Bauer, M., Semerad, R., and Kinder, H. (1999). "YBCO films on metal substrates with biaxially aligned MgO buffer layers," *IEEE Trans. Appl. Supercond.* **9**, 1502–1505.
- Brese, N. E. and O'Keeffe, M. (1991). "Bond-valence parameters for solids," *Acta Crystallogr.* **47**, 192–197.
- Brown, I. D. and Altermatt, D. (1985). "Bond-valence parameters obtained from a systematic analysis of the inorganic crystal-structure database," *Acta Crystallogr.* **41**, 244–247.
- Buttner, R. H., and Maslen, E. N. (1993). "Structural parameters and electron difference density in Y_2BaCuO_5 ," *Acta Crystallogr.* **49**, 62–66.
- Feenstra, T., Lindemer, T. B., Budai, J. D., and Galloway, M. D. (1991). "Effect of oxygen pressure on the synthesis of $\text{YBa}_2\text{Cu}_3\text{O}_{7-x}$ thin-films by post-deposition annealing," *J. Appl. Phys.* **69**, 6569–6585.
- Feenstra, R. (1999). "Method for making high-critical-current-density $\text{YBa}_2\text{Cu}_3\text{O}_7$ superconducting layers on metallic substrates," U.S. Patent No. 5,972,847 (October 26, 1999).
- Fjellvag, H., Karen, P., and Kjekshus, A. (1987). "Structural-properties and phase-transitions of Y_2BaCuO_5 and $\text{YBa}_2\text{Cu}_3\text{O}_{9-x}$," *Acta Chem. Scand.* (1947-1973) **41**, 283–293.
- Foltyn, S. R., Tiwari, P., Dye, R. C., Le, M. Q., and Wu, X. D. (1993). "Pulsed-laser deposition of thick $\text{YBa}_2\text{Cu}_3\text{O}_{7-x}$ films with J_c -greater-than-1 MA/CM²," *Appl. Phys. Lett.* **63**, 1848–1850.
- Goyal, A., Lee, D. F., Lost, F. A., Specht, E. D., Feenstra, R., Paranthaman, M., Cui, X., Lu, S. W., Martin, P. M., Kroeger, D. M., Christen, D. K., Kang, B. W., Norton, D. P., Park, C., Verebelyi, D. T., Thompson, J. R., Williams, R. K., Aytug, T., and Cantoi, C. (2001). "Recent progress in the fabrication of high- J_c tapes by epitaxial deposition of YBCO on RABiTS," *Physica C* **357**, 903–913.
- Goyal, A., Paranthaman, M. P., and Schoop, U. (2004). "The RABiTS approach: Using rolling-assisted biaxially textured substrates for high-performance YBCO superconductors," *MRS Bull.* **29**, 552–561.
- Hazen, R. M., Finger, L. W., Angel, R. A., Prewitt, C. T., Ross, N. L., Mao, H. K., and Hadjidakos, C. G. (1987). "Crystallographic description of phases in the Y–Ba–Cu–O superconductor," *Phys. Rev. B* **35**, 7238–7241.
- Hsu, R., Maslen, E. N., and Ishizawa, N. (1996). "A synchrotron X-ray study of the electron density in Y_2BaCuO_5 ," *Acta Crystallogr.* **52**, 569–572.
- Hunter, B. A., Town, S. L., Davis, R. L., Russell, G. J., and Taylor, K. N. R. (1989). "Neutron-scattering study of the structure of Y_2BaCuO_5 at 294 K and 77 K," *Physica C* **161**, 594–597.
- ICDD (1987). "Powder Diffraction File," International Centre for Diffraction Data, edited by Frank McClune, 12 Campus Boulevard, Newtown Square, PA 19073–3272.
- Iijima, Y., Kakimoto, K., Yamada, Y., Izumi, T., Saitoh, T., and Shiohara, Y. (2004). "Research and development of biaxially textured IBAD-GZO templates for coated superconductors," *MRS Bull.* **29**, 564–571.
- Larson, A. C. and von Dreele, R. B. (1985). "GSAS—General Structure Analysis System," U.S. Government Contract (W-7405-ENG-36), Los Alamos National Laboratory, U.S. Department of Energy.
- Malozemoff, A. P., Annavaou, S., Fritzsche, L., Li, Q., Prunier, V., Rupich, M., Thieme, C., Zhang, W., Goyal, A., Paranthaman, M., and Lee, D. F. (2000). "Low-cost YBCO coated conductor technology," *Supercond. Sci. Technol.* **13**, 376–473.
- McIntyre, P. C., Cima, M. J., and Roshko, A. (1995). "Epitaxial nucleation and growth of chemically derived $\text{Ba}_2\text{YCu}_3\text{O}_{7-x}$ thin-films on (001) SrTiO_3 ," *J. Appl. Phys.* **77**, 5263–5272.
- Michel, C. and Raveau, B. (1982). "The oxides A_2BaCuO_5 (A = Y, Sm, Eu, Gd, Dy, Ho, Er, Yb)," *J. Solid State Chem.* **43**, 73–80.
- Paranthaman, M., Goyal, A., List, F. A., Specht, E. D., Lee, D. F., Martin, P. M., He, Q., Christen, D. K., Norton, D. P., Budai, J. D., and Kroeger, D. M. (1997). "Growth of biaxially textured buffer layers on rolled-Ni substrates by electron beam evaporation," *Physica C* **275**, 266–272.
- Paranthaman, M., Park, C., Cui, X., Goyal, A., Lee, D. F., Martin, P. M., Chirayil, T. G., Verebelyi, D. T., Norton, D. P., Christen, D. K., and Kroeger, D. M. (2000). " $\text{YBa}_2\text{Cu}_3\text{O}_{7-x}$ -coated conductors with high engineering current density," *J. Mater. Res.* **15**, 2647–2652.
- Paranthaman, M. P. and Izumi, T. (2004). "High performance YBCO-coated superconductor wires," *MRS Bull.* **29**, 533–536.
- Reade, R. P., Berdahl, P., Russo, R. E., and Garrison, S. M. (1992). "Laser deposition of biaxially textured yttria-stabilized zirconia buffer layers on polycrystalline metallic alloys for high critical current Y–Ba–Cu–O thin films," *Appl. Phys. Lett.* **61**, 2231–2233.
- Rietveld, H. M. (1969). "A profile refinement method for nuclear and magnetic structures," *J. Appl. Crystallogr.* **2**, 65–71.
- Ross, N. L., Angel, R. J., Finger, L. W., Hazen, R. M., and Prewitt, C. T. (1987). "Oxygen-defect perovskites and the 93 K superconductor," *ACS Symp. Ser.* **351**, 164–172.
- Roth, R. S., Rawn, C. J., Whittler, J. D., Chiang, C. K., and Wong-Ng, W. (1989). "Phase equilibria and crystal chemistry in the quaternary system Ba–Sr–Y–Cu–O in air," *J. Am. Ceram. Soc.* **72**, 395–399.
- Rupich, M. W., Verebelyi, D. T., Zhang, W., Kodankandath, T., and Liopen, X. (2004). "Metalorganic deposition of YBCO films for second-generation high-temperature superconductor wires," *MRS Bull.* **29**, 572–578.
- Salinas-Sanchez, A., Garcia-Munoz, J. L., Rodriguez-Carvajal, J., Saez-Puche, R., and Martinez, J. L. (1992). "Structural characterization of R_2BaCuO_5 (R = Y, Lu, Yb, Tm, Er, Ho, Dy, Gd, Eu and Sm) oxides by X-ray and neutron-diffraction," *J. Solid State Chem.* **100**, 201–211.
- Sato, S. and Nakada, I. (1989). "Structure of Y_2BaCuO_5 —A refinement by single-crystal X-ray diffraction," *Acta Crystallogr., Sect. C: Cryst. Struct. Commun.* **45**, 523–525.
- Selvamanickam, V., Xie, Y., Reeves, J., and Chen, Y. (2004). "MOCVD-based YBCO-coated conductors," *MRS Bull.* **29**, 579–582.
- Shaked, H., Etedgui, H., Gavra, Z., Melamud, M., Johnson, J. R., Reilly, J. J., and Pinto, H. (1993). "Crystal-structure and magnetic-properties of $\text{DuY}_2\text{BaCuO}_5$ ($u=0.00, 0.61, 1.31$)," *J. Alloys Compd.* **194**, 13–17.
- Shannon, R. D. (1976). "Revised effective ionic-radii and systematic studies of interatomic distances in halides and chalcogenides," *Acta Crystallogr.* **32**, 751–767.
- Solovyov, V. F., Wiesmann, H. J., Suenaga, M., and Feenstra, R. (1998). "Thick $\text{YBa}_2\text{Cu}_3\text{O}_7$ films by postannealing of the precursor by high rate e-beam deposition on SrTiO_3 substrates," *Physica C* **309**, 269–274.
- Usoskin, A., and Freyhardt, H. C. (2004). "YBCO-coated conductors manufactured by high-rate pulsed laser deposition," *MRS Bull.* **29**, 583–589.
- Watkins, S. F., Fronczek, R. R., Wheelock, K. S., Goodrich, R. G., Hamilton, W. O., and Johnson, W. W. (1988). "Structure of Y_2BaCuO_5 ," *Acta Crystallogr., Sect. C: Cryst. Struct. Commun.* **44**, 3–6.
- Wong-Ng, W., Kuchinski, M. A., McMurdie, H. F., and Paretzkin, B. (1989). "X-ray powder diffraction characterization of BaR_2CuO_5 , (R = yttrium and the lanthanides) and related compounds," *Powder Diffr.* **4**, 2–8.
- Wong-Ng, W., Piermarini, G., and Gallas, M. (1995). "X-ray diffraction study of $\text{BaNd}_2\text{CuO}_5$ under high pressure," *Adv. X-Ray Anal.* **38**, 741–747.
- Wu, L., Zhu, Y., Solovyov, V. F., Wiesmann, H. J., Moodenbaugh, A. R., Sabatini, R. L., and Suenaga, M. (2001). "Nucleation band growth of $\text{YBa}_2\text{Cu}_3\text{O}_x$ on SrTiO_3 and CeO_2 by a BaF_2 postdeposition reaction process," *J. Mater. Res.* **16**, 2869–2884.
- Yoshizumi, M., Seleznev, I., and Cima, M. J. (2004). "Reactions of oxyfluoride precursors for the preparation of barium yttrium cuprate films," *Physica C* **403**, 191–199.